NAVAL POSTGRADUATE SCHOOL
Monterey, California

THESIS

RESPONSE OF THE UPPER
OCEAN TO HURRICANE ELOISE

by

Laurence Victor Friese

December 1977

Thesis Advisors: R. L. Elsberry
                    D. F. Leipper

REPORT DOCUMENTATION PAGE

**READ INSTRUCTIONS
BEFORE COMPLETING FORM**

1. REPORT NUMBER	2. GOVT ACCESSION NO.	3. RECIPIENT'S CATALOG NUMBER

4. TITLE (and Subtitle)

Response of the Upper Ocean to Hurricane Eloise.

5. TYPE OF REPORT & PERIOD COVERED

Master's Thesis, December 1977

6. PERFORMING ORG. REPORT NUMBER

7. AUTHOR(s)

Laurence Victor/Friese

8. CONTRACT OR GRANT NUMBER(s)

9. PERFORMING ORGANIZATION NAME AND ADDRESS

Naval Postgraduate School
Monterey, California 93940

10. PROGRAM ELEMENT, PROJECT, TASK AREA & WORK UNIT NUMBERS

11. CONTROLLING OFFICE NAME AND ADDRESS

Naval Postgraduate School
Monterey, California 93940

12. REPORT DATE

December 1977

13. NUMBER OF PAGES

53

14. MONITORING AGENCY NAME & ADDRESS(If different from Controlling Office)

Naval Postgraduate School
Monterey, California 93940

15. SECURITY CLASS. (of this report)

Unclassified

15a. DECLASSIFICATION/DOWNGRADING SCHEDULE

16. DISTRIBUTION STATEMENT (of this Report)

Approved for public release; distribution unlimited.

17. DISTRIBUTION STATEMENT (of the abstract entered in Block 20, if different from Report)

18. SUPPLEMENTARY NOTES

19. KEY WORDS (Continue on reverse side if necessary and identify by block number)

Hurricane
Air-Sea Interaction
Mixed Layer Depth
Internal Waves

20. ABSTRACT (Continue on reverse side if necessary and identify by block number)

Buoy data provided clear evidence of mixed layer deepening and an internal wave caused by Hurricane Eloise, September 1975. Logarithmic temperature profiles below an isothermal mixed layer were assumed and used to model thermocline oscillation and heat budget calculation as influenced by Eloise over a 21-day period. Results show that prior to the arrival of Eloise at the buoy, the average mixed layer depth was about 33m. As the winds increased due to hurricane approach, the mixed layer deepened steadily to about 42m before upwelling to approximately 22m. The thermocline then underwent three

DD FORM 1473 EDITION OF 1 NOV 65 IS OBSOLETE
1 JAN 73
(Page 1)   S/N 0102-014-6601 |

251 450

Block 20 - ABSTRACT (Cont.)

distinctly large oscillations of inertial periodicity, while the mixed layer continued to deepen. The post-storm average mixed layer depth was about 52m. Values of mixed layer depth were concluded to be accurate to within 2m. Vertical velocities, calculated first by assuming zero horizontal temperature advection in the material derivative equation and second by finding the mass transport necessary to balance the heat budget, show that in the upper 500m of the water column downward vertical motion of 1m/hr or less prevailed during storm approach, followed by upward vertical velocity as great as 5.35m/hr during the 12 hr immediately following hurricane passage followed by downward vertical velocity during the large thermocline oscillations.

Response of the Upper
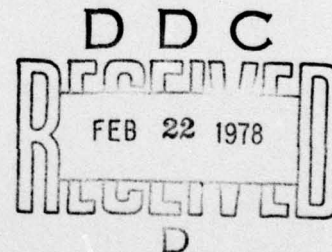
Ocean to Hurricane Eloise

by

Laurence Victor Friese
Lieutenant Commander, United States Navy
B.S., University of Washington, 1965

Submitted in partial fulfillment of the
requirements for the degree of

MASTER OF SCIENCE IN METEOROLOGY AND OCEANOGRAPHY

from the

NAVAL POSTGRADUATE SCHOOL
December 1977

D D C

FEB 22 1978

D

Author _____
For Laurence V. FRIESE

Approved by: _____
Thesis Advisor

_____
Co-Advisor and Chairman, Department of Oceanography

_____
Dean of Science and Engineering

ABSTRACT

Buoy data provided clear evidence of mixed layer deepening and an internal wave caused by Hurricane Eloise, September 1975. Logarithmic temperature profiles below an isothermal mixed layer were assumed and used to model thermocline oscillation and heat budget calculation as influenced by Eloise over a 21-day period. Results show that prior to the arrival of Eloise at the buoy, the average mixed layer depth was about 33m. As the winds increased due to hurricane approach, the mixed layer deepened steadily to about 42m before upwelling to approximately 22m. The thermocline then underwent three distinctly large oscillations of inertial periodicity, while the mixed layer continued to deepen. The post-storm average mixed layer depth was about 52m. Values of mixed layer depth were concluded to be accurate to within 2m. Vertical velocities, calculated first by assuming zero horizontal temperature advection in the material derivative equation and second by finding the mass transport necessary to balance the heat budget, show that in the upper 500m of the water column downward vertical motion of 1m/hr or less prevailed during storm approach, followed by upward vertical velocity as great as 5.35m/hr during the 12 hr immediately following hurricane passage followed by downward vertical velocity during the large thermocline oscillations.

4

TABLE OF CONTENTS

LIST OF TABLES

LIST OF FIGURES

ACKNOWLEDGEMENT

Although first-order acknowledgement must go to my thesis advisor
and co-advisor Drs. Russ Elsberry and Dale Leipper, I wish to also thank
not only LCDR Norm Camp, U.S. Navy, who was always so very sincere and
generous in sharing his knowledge, but also the many faculty members of
the Naval Postgraduate School who always welcomed my questions. Finally,
I am grateful to the workers at the NOAA Data Buoy Office for collecting
and disseminating the unique set of data which was studied in this
thesis, and for the helpful explanations I got from NDBO in several
telephone conversations regarding the data.

I. INTRODUCTION

By a stroke of luck, the eye of Hurricane Eloise on 23 September 1975 passed over the National Oceanic and Atmospheric Administration's EB-10-- a forty-foot diameter data buoy anchored in the Gulf of Mexico. Numerous instruments, both on the buoy itself and attached to the line anchoring the buoy to the floor of the Gulf, gathered atmospheric and oceanographic data throughout the three days before and 18 days after hurricane passage. The purpose of this thesis is to study the response of the upper ocean to Hurricane Eloise and to report the results obtained.

The mechanisms that produce changes in ocean thermal structure in the wake of severe tropical cyclones have been studied for some time. In addition to the heat loss to the atmosphere, the oceanic processes of vertical and horizontal advection plus turbulent mixing at the top of the thermocline have been shown to contribute to cooling of the upper layers in the ocean. Jordan [1964] reasoned that for typical mixed layer depths, large temperature decreases could not be due to the heat loss to the atmosphere but must originate from the thermocline layers through vertical fluxes. Leipper [1967] reported what is probably the best-known survey of oceanic thermal response. Black and Mallinger [1972] combined airborne expendable bathythermograph and conventional data to study the effects of hurricane Ginger. Although a common shortcoming of the observational studies has been the sparsity of coincident before-after soundings allowing determination of the changes due to the hurricane, Fedorov [1973] used before and after soundings at ocean weather station (OWS) Tango to calculate the temperature changes due to the passage of

9

14 typhoons. Elsberry et al. [1974] developed an empirical hurricane boundary layer model for hurricane-ocean interaction studies. This model, which was used recently to drive a mixed layer model of the upper ocean [Elsberry et al., 1976] to simulate the thermal response induced by a hurricane, emphasized the role of vertical fluxes by incorporating a mixing-layer model similar to Kraus and Turner [1967] and Denman [1973]. In this thesis, logarithmic temperature profiles as suggested by Tully [1953] were used to estimate the temperature structure. These profiles were used to predict the depth of the mixed layer and to balance the heat budget in the wake of the storm. Oscillations of the thermocline predicted by Geisler [1970], documented by Black [see Sheets 1974] and modeled by Grigsby [1975] were observed. The heat budget was calculated producing the horizontal and vertical velocities necessary to account for the observed temperature changes.

II. PROCEDURE

A. DATA

The buoy EB-10, located at 27°28'N, 88°01'W, in 1313 fathoms of water, gathered atmospheric data plus the temperature and hydrostatic pressure of the water near the surface and at three subsurface depths in the Gulf of Mexico during the passage of Hurricane Eloise. These data were published by the NOAA Data Buoy Office in a report titled Data Report: Buoy Observations During Hurricane Eloise (September 19 to October 11, 1975, November 7, 1975) (Withee and Johnson, 1975).

B. TEMPERATURE PROFILES

To study the nature and extent of influence of a hurricane on the ocean, having the temperature of the sea water before, during and after

hurricane passage at all depths would be optimal. But the system avail-
able provided temperatures with a maximum frequency of only once per hour
and recorded them only near the surface and at three sub-surface depths--
approximately 50, 200 and 500 meters. These are only nominal depths be-
cause of the vertical wandering of 10-12 meters due to periodic pulling
on the mooring line by the drifting buoy in the high winds and accompa-
nying waves. The near-surface temperature value was measured at a depth
of two meters and will be referred to throughout this thesis as the
surface temperature.

The first goal of this thesis was to estimate the temperature at all
depths for any observational time knowing the temperature at only the
surface and three subsurface depths. Estimates of the above type were
made for 170 different observation times throughout the 21-day period
bracketing the passage of the storm over EB-10. A temperature structure
of the water was also estimated by the NOAA Data Buoy Office (NDBO)
[Withee and Johnson, 1975, page B-30]. A portion of NDBO's plot is shown
in Figure 1; the surface and three subsurface temperature values are
written for each observation time at the depth of the measurements. The
isotherms shown in Figure 1 were drawn assuming a linear temperature
change with depth. Black and Withee [1976] and Price [1977] used these
same data, and estimated the temperature change with depth for all times
with gradients based on a single AXBT dropped near EB-10 on the day prior
to Eloise's passage over the buoy. In this thesis the positions of iso-
therms, as well as the depth of the thermocline, were calculated at each
of the 170 observation times assuming a logarithmic temperature change
with increasing pressure defined by the three observed subsurface temper-
ature values. Each logarithmic curve was then matched to a vertical line

11
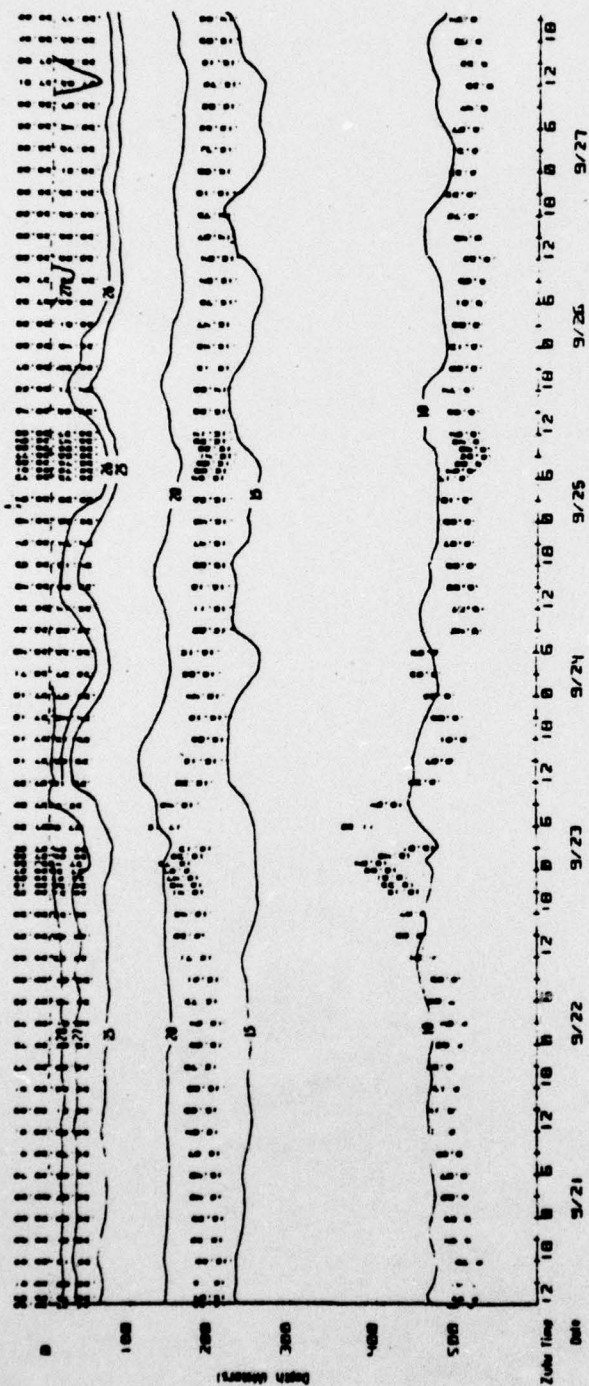
FIGURE 1. Contoured time series representation of sea temperature (°C) from EB-10 during Hurricane Eloise. Isotherm position as determined by NDBO [Withee and Johnson, 1975, page B-30]. Numbers printed at surface and three subsurface depths are, for each observation time, temperature values observed at sensor depths. Note that sensor depths varied up and down in response to buoy motion.

12

representing an isothermal mixed layer having temperature equal to the surface temperature observed at the respective observation time. This procedure assumes the three subsurface temperatures were within the thermocline. After passage of Eloise, the nominal 50 m observations were occasionally equal to the surface temperature, indicating that the mixed layer was greater than 50 m. In these cases only the two lowest subsurface observations are available to define the logarithmic temperature profile.

1. Procedure For Calculating The Logarithmic Temperature Profile
    Below The Mixed Layer At Any Given Observation Time

At 0900 GMT, 21 September 1975, the data provided by EB-10 indicated that the three following subsurface temperatures existed at the given pressures:

T_{ob}	p	ln p
25.784°C	6.427kg/cm^2	1.8605
15.677	22.986	3.1349
9.055	52.148	3.9541

where T_{ob} is the observed temperature and p is pressure. A least-squares linear regression was calculated using the natural logarithm of pressure (ln p) versus T_{ob}.

Figure 2 shows graphically the best-fit curve through the three sets of values being considered. The slope and intercept of the regression curve for this case were calculated as -0.125 and 5.092 respectively. That is, the equation relating pressure and temperature is

$$\ln p = -0.125T + 5.092 \ . \qquad (1)$$

A similar equation was calculated for each of the 170 observation times using the Naval Postgraduate School IBM 360 computer

13
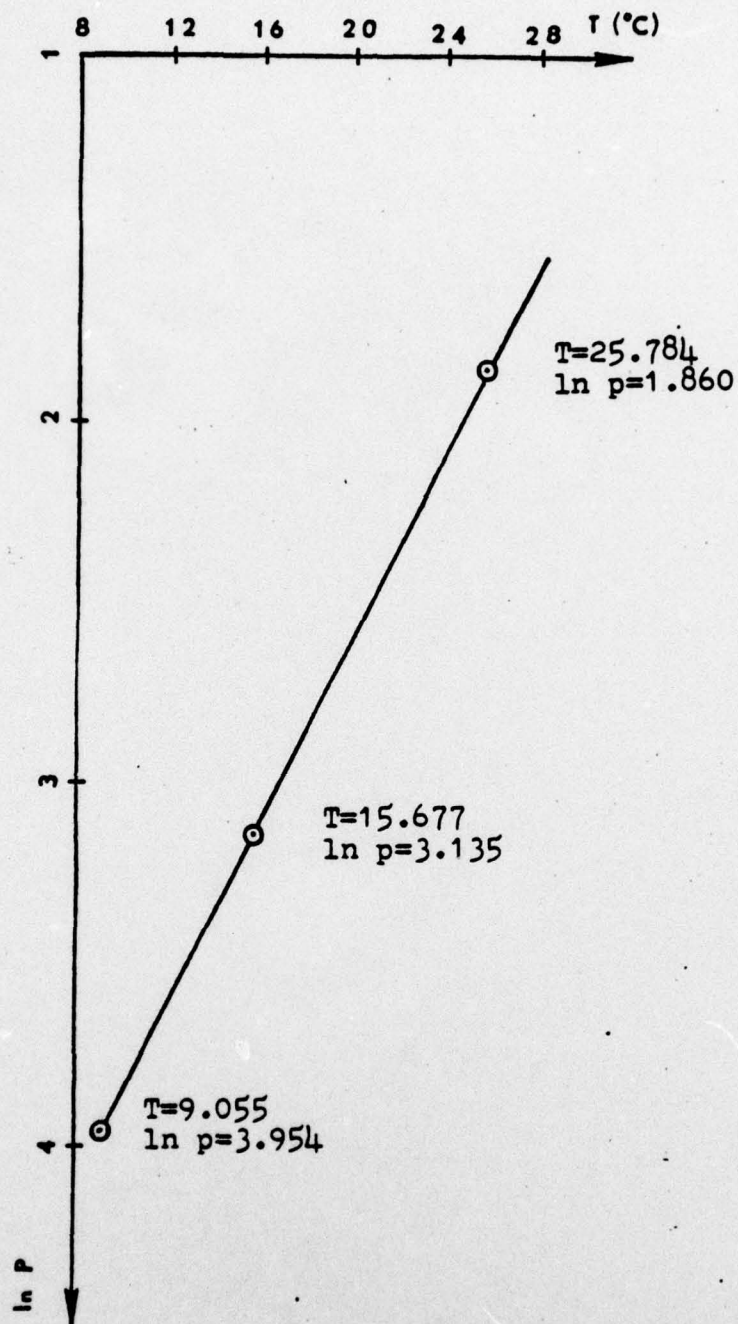
FIGURE 2. Example best-fit linear regression curve obtained from subsurface temperature and pressure values. This example is for the observation time of 0900 GMT, 21 September 1975. Curve has a slope of -0.125 and an intercept of 5.092.

subroutine to calculate linear regressions. The slopes m and intercepts b specify the thermocline temperature profiles throughout the 21 days under consideration. The general equation is

$$\ln p = mT + b . \tag{1a}$$

To estimate the accuracy of equation (1), the three values of the logarithm of pressure used in the regression can be used in equation (1) to calculate the regression temperatures (T_r). The following information was found:

p (kg/cm^2)	T_{ob} (°C)	T_r(°C)	Error = $T_r - T_{ob}$ (°C)
6.427	25.819	25.804	0.015
22.986	15.677	15.627	-0.050
52.148	9.055	9.085	0.030

The largest error in temperature for this observation time is -0.05°C, and is associated with the middle of the three subsurface temperature measurements--a characteristic of drawing the best linear fit through the three points. According to NDBO, the accuracy of the temperature sensors was 0.05°C for the surface and two deepest subsurface sensors, and 0.2°C for the sensor located near the 50 m depth. Consequently the logarithmic profile technique fit the data at the three levels within the expected accuracy of the temperature observations. A more complete description of temperature profile errors will be given later.

2. Procedure For Calculating The Temperature and Depth of The Mixed Layer At Any Given Observation Time

The next step in the procedure was to match the observed surface temperature with the thermocline profile given by equation (1). The surface temperature at 0900 GMT, 21 September 1975 was observed to be 28.819°C. Entering this value for temperature in equation (1) gives

15

p = 4.406. Using this calculated pressure value and assuming an isother-
mal mixed layer, the complete temperature profile can now be drawn from
the surface to the point of the deepest observation. This complete pro-
file for 0900 GMT, 21 September 1975, is shown in Figure 3A. Figure 3B
shows the same profile, except that pressure was plotted linearly vice
logarithmically.

Figure 3C shows the profile assuming a linear temperature change
in depth as used by the NOAA Data Buoy Office when plotting Figure 1.
The profile in Figure 3B appears to be a much more realistic representa-
tion of conditions observed daily in the subtropical oceans. The point
of intersection of the vertical isothermal line with the regression curve
in Figure 3A or 3B is defined in this thesis as the hydrostatic pressure
at the bottom of the mixed layer, i.e. at the top of the thermocline.

Throughout this thesis, pressure p (kg/cm^2) was converted to
depth z (m) according to an approximation algorithm suggested by NDBO
for the subsurface (more than 40m) data

$$z = (9.75p - 10) \ . \qquad\qquad (2)$$

Hence the mixed layer depth can be found for 0900 GMT, 21 September 1975
by substituting p = 4.406 into equation (2) giving MLD = 33.0m.

Temperature profiles extending from the surface to the deepest
observation, as well as the respective mixed-layer depths, were calcu-
lated for all 170 observation times as in the example above. A plot of
MLD vs time was made for studying the motion of the thermocline and the
deepening of the mixed layer during the three days before and 18 days
after the passage of Hurricane Eloise over EB-10. This plot will be
presented and discussed in a later section.
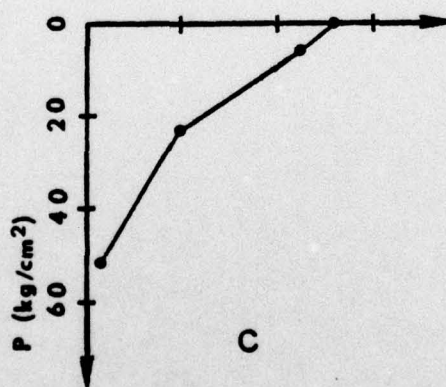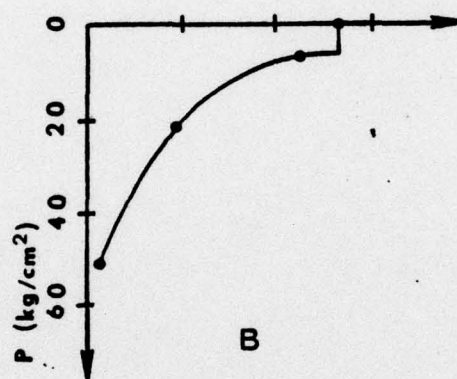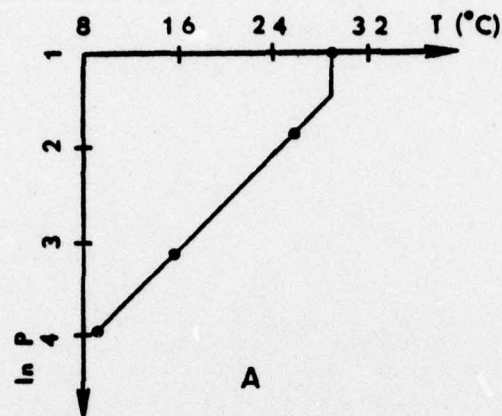
FIGURE 3. Derived temperature profile from surface to point of deepest observation for the observation time of 0900 GMT, 21 September 1975. Pressure is plotted logarithmically in A and linearly in B; C shows the profile for this observation time assumed by NOAA Data Buoy Office. An isothermal mixed layer was assumed, i.e. a vertical line was drawn from surface temperature to point of intersection with regression curve.

17

3. Procedure For Calculating The Position of Isotherms

The depth z of, e.g., the 25°C isotherm, can be found for 0900 GMT, 21 September 1975 by letting $T = 25$ in equation (1) and solving for p and then substituting for p into equation (2). Doing this gives a depth of 59.3m for the 25° isotherm at this time. For this thesis depths were thus calculated for the 25, 23, 21, 18, 15, 12 and 9° isotherms at all 170 observation times. A plot of isotherm depth versus time was made for studying isotherm motion during the three days before and 18 days after the passage of Hurricane Eloise over EB-10. This plot will be compared to a similar plot made by NOAA's Data Buoy Office shown in Figure 1 above.

C. CALCULATING THE HEAT BUDGET

The procedure used in this thesis to calculate the heat budget was a simplified one. The problem was unique in that the heat budget was examined over a period of time with large amplitude oscillations on the thermocline. The time change of heat content (cal/cm^2) of a column of water under the buoy 500 meters deep and one square centimeter in cross section is related to the time change of average temperature obtained from the profiles derived above. That is,

$$\Delta H - \rho C_p \, z \, \Delta T_{av} \qquad (3)$$

where H = heat in cal/cm^2

ρ = density of water $\doteq 1$ gm/cm^3

C_p = heat capacity of water at constant pressure $\doteq 1$ $cal/gm/°C$

z = the height (cm) of the column of water one square centimeter in cross-section

T_{av} = average temperature (°C) of the column of water, as calculated using the logarithmic regression curves discussed earlier

In terms of time derivatives equation (3) becomes

$$\frac{\partial H}{\partial t} = \rho C_p \; z \; \frac{\partial Tav}{\partial t} \; . \tag{3a}$$

and will be called the storage term. If the temperature change is measured in degrees Celsius per hour, the storage term will have units of $cal/cm^2/hr$.

From the first law of thermodynamics, two mechanisms were considered as changing the heat content of the column--the net flux of latent, sensible and radiative heat transfer across the sea surface, and heat flux by three dimensional advection. The formulae used [see Husby and Seckel, 1975] for obtaining the net flux of latent, sensible and radiative heat (Q_n) was

$$Q_n = Q_s - Q_b - Q_e - Q_c \tag{4}$$

where Q_s , the solar insolation term, was measured directly by EB-10, and

$$Q_b = 1.14 \times 10^{-7} (273.16 + T_w)^4$$
$$\times (0.39 - 0.05 e_a^{1/2})(1 - 0.6C^2) \; ,$$
$$Q_e = 3,767 C_d (0.98 e_w - e_a) W \; , \text{ and}$$
$$Q_c = 2.488 C_p (T_w - T_a) W$$

where

e_a is the saturation vapor pressure (mb) of the atmosphere at the height of ten meters calculated using the Goff-Gratch formulation of the Clausius-Clapeyron equation with the dewpoint temperature as the entering argument

e_w is the saturation vapor pressure (mb) of the atmosphere at the sea surface calculated similar to e_a except using sea surface temperature as the entering argument

C_d is the nondimensional drag coefficient equal to $(0.63 + 0.66 \times W) \times 10^{-3}$, [Smith and Banke, 1975]

T_a is the temperature of the air in degrees Celsius

T_w is the temperature of the water in degrees Celsius

W is the wind speed in meters per second

and C, (the fraction of sky covered by clouds),
 is 0.80 from 1200 GMT 20 SEP to 1800 GMT 22 SEP,
 1.00 from 2100 GMT 22 SEP to 1200 GMT 23 SEP,
 0.85 from 1500 GMT 23 SEP to 1200 GMT 24 SEP,
 0.75 from 1500 GMT 24 SEP to 1100 GMT 25 SEP, and
 0.50 from 1200 GMT 25 SEP to 1200 GMT 26 SEP.

Herein Q_n (cal/cm^2/hr) is called the surface flux term.

The 500-meter deep column was then divided into five layers, each 100 meters deep, and vertical and horizontal velocities were calculated that satisfied the heat budget. The first attempt to obtain these velocities was the commonly used assumption that the material derivative of temperature was zero and that there was no horizontal temperature gradient. Starting with the equation

$$\frac{dT}{dt} = 0 = \frac{\partial T}{\partial t} + V_H \cdot \nabla T + w \frac{\partial T}{\partial z} \tag{5}$$

setting $V_H \cdot \nabla T = 0$, and solving for w gives

$$w = - \frac{\partial T}{\partial t} \Big/ \frac{\partial T}{\partial z} . \tag{5a}$$

Both $\partial T/\partial t$ and $\partial T/\partial z$ were directly available from the 170 temperature profiles obtained as discussed earlier. The values of w were thus computed at 100, 200, 300, 400 and 500 meters. These values of w were related to the vertical mass flow rate into or out of each layer of the column by the equation

$$M_z = \rho w \tag{6}$$

where M_z is directed positive upward in accordance with the positive z axis.

20

From the continuity equation the horizontal mass flux into or out of the column was calculable from the vertical mass fluxes. The net horizontal mass flow must compensate for the difference in vertical mass fluxes. Let

$$M_H = \int_{z_B}^{z_T} \rho V_H \, dz \tag{7}$$

where M_H = the horizontal transport of mass per unit width of vertical surface

V_H = the horizontal velocity,

z_B and z_T = the depths in meters at the bottom and top of the column.

For incompressible flow in a constant-density fluid,

$$\int_{z_B}^{z_T} \nabla \cdot \rho V_H \, dz + \int_{z_B}^{z_T} \rho \frac{\partial w}{\partial z} \, dz = 0$$

Combined with equations (6) and (7), the above equation gives

$$M_H = M_{z_B} - M_{z_T} . \tag{8}$$

Horizontal mass flow is defined as positive if directed out of the column.

There was some question whether the w's obtained using equation (5a) could be accurate, since the assumption of zero horizontal temperature advection seemed unlikely. This was checked by using the calculated vertical velocities and the storage and surface flux terms in the heat budget. The total heat flux (THF) across all faces of a water column due to three-dimensional advection was defined as

$$THF = M_{z_B} C_p T_B - M_{z_T} C_p T_T - M_H C_p T_{av} \tag{9}$$

21

where T_{av} is the average temperature of a 100m-deep column of water with cross-section equal to one square centimeter, T_B and T_T the temperatures at the bottom and top respectively of the same 100m-deep column, and M_{z_B}, M_{z_T} and M_H are the mass transports across the bottom, top and horizontal faces, respectively, of the column. Substituting equation (8) into (9) and adding the storage and surface flux terms give the full equation used in analyzing the heat budget,

$$\frac{\partial H}{\partial t} = \rho C_p z \frac{\partial T_{av}}{\partial t} = C_p M_{z_B} (T_B - T_{av}) + C_p M_{z_T} (T_{av} - T_T) - Q_n .$$

Rearranging provides the equation

$$M_{z_B} = \left[-\frac{1}{C_p} \frac{\partial H}{\partial t} - M_{z_T}(T_T - T_{av}) - \frac{Q_n}{C_p} \right] / (T_{av} - T_B) \qquad (10)$$

Combining equation (10) with equation (6) gives

$$w = M_z/\rho = \left\{ \left[-\frac{1}{C_p} \frac{\partial H}{\partial t} - M_{z_T}(T_T - T_{av}) - \frac{Q_n}{C_p} \right] \Big/ (T_{av} - T_B) \right\} / \rho \qquad (10a)$$

While M_{z_T} was considered to be, by the kinematic boundary condition, equal to zero at the sea surface, Q_n was considered to be equal to zero at all depths except the surface. Because the M_{z_B}, M_{z_T} and M_H are mean quantities averaged over the time increment between observations, the contribution of turbulent motions on smaller time scales is not considered.

As an example consider the problem of calculating the vertical velocity of 100 m as given, first, by equation (5a) and second by equation (10a) for the observation time (t_{ob}) of 1500 GMT, 23 September 1975:

1. <u>Calculation of Vertical Velocities Assuming Zero Horizontal Temperature Advection</u>

The values of slope m, intercept b, pressure at the bottom of the mixed layer p_{MLD} and MLD in the following table were obtained from the respective regression curves plus equations (1a) and (2), while the surface temperature T_{sfc} was obtained from the published buoy data for 23 September 1975.

t_{ob} GMT	m	b	p_{MLD} (kg/cm^2)	MLD (m)	T_{sfc} (°C)	T_{100m} (1C)
1200	-0.152	5.345	3.331	22.47	27.226	19.205
1500	-0.153	5.334	3.280	21.98	27.166	19.072
1800	-0.145	5.253	3.733	26.40	27.166	19.532

The numerator of equation (5a), refers to a single level, say 100m, and is evaluated at 1500 GMT, using a centered finite difference, as

$$(19.532 - 19.205)\text{°C}/6\text{hr}.$$

The denominator in equation (5a) was approximated by using the 1500 GMT regression temperature profile over an increment one meter above and below the 100 meter level. Thence the calculated value of vertical velocity w was -0.91m/hr. Similar calculations produced the values for this method's vertical velocities at each of the deeper levels. The left-hand set of arrows in Figure 4 shows the values calculated.

2. <u>Calculation of Vertical Velocities Not Assuming Zero Horizontal Temperature Advection</u>

To solve for the mass transport at the 100 meter level for 1500 GMT 23 September 1975 using equation (10), we must calculate the average temperature in the upper 100m of the ocean in the vicinity of the buoy for each of the three observation times listed in paragraph 1

23
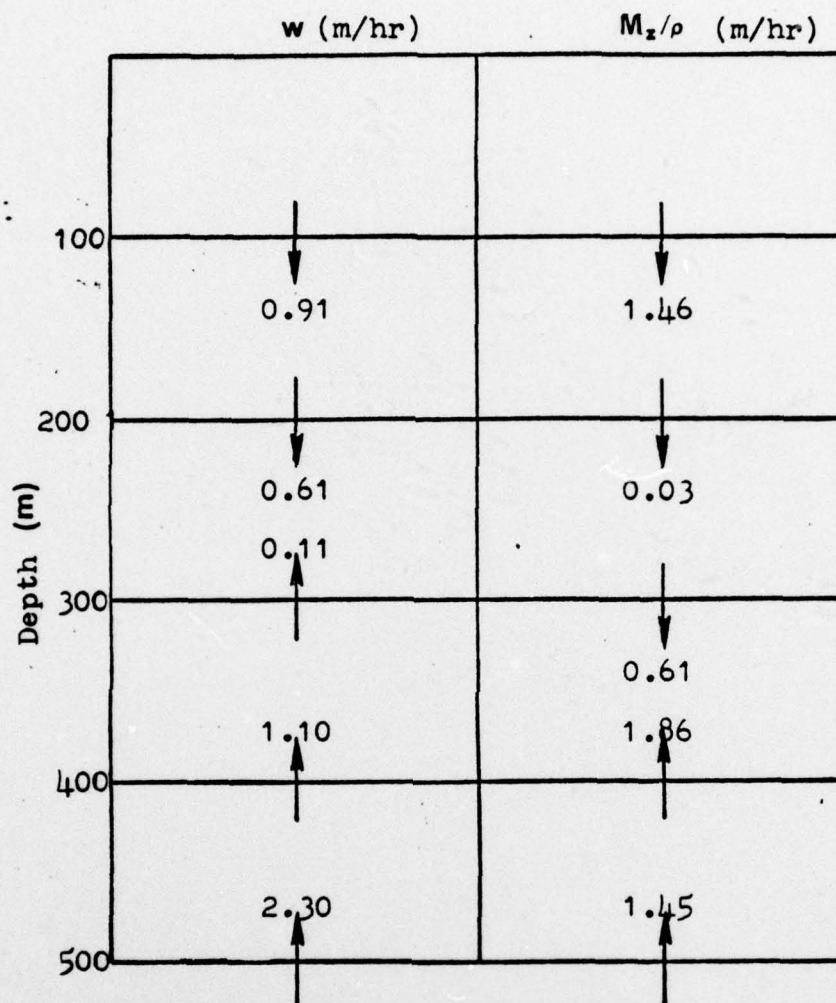
FIGURE 4. Vertical velocities at 100m depth increments in the left column were obtained using equation (5a), i.e. assuming zero horizontal temperature advection. Values of M_z/ρ in right column were obtained using equation (10a), i.e. not assuming zero horizontal temperature advection. These vertical velocities are for the observation time of 1500 GMT, 23 September 1975.

above. Assume the general equation is

$$(T_{av})_{0 \to 100m} = [MLD(T_{sfc}) + (100-MLD)(T_{av})_{MLD \to 100m}]/100 \qquad (11)$$

The average temperature for any layer of water having a logarithmic temperature profile and lying between pressure surfaces p_B and p_T is given by

$$(T_{av})_{p_T \to p_B} = \frac{1}{p_B - p_T} \int_{p_T}^{p_B} T(p)\,dp \qquad (12)$$

Combining equation (1a) with (13) gives

$$(T_{av})_{p_T \to p_B} = \frac{1}{p_B - p_T} \int_{p_T}^{p_B} (\frac{\ln p - b}{m})\,dp =$$

$$m(p_T - p_B)[p_B(\ln p_B - p_B - bp_B) - p_T(\ln p_T - p_T - bp_T)] \qquad (13)$$

Equation (13) can be used to get the average temperature from the bottom of the mixed layer to the 100m depth, which for 1200 GMT, 23 September turns out to be 22.422°C. This value can then be used in equation (11) to get the average temperature for the layer 0-100m, which is 23.501°C in this example. In an analogous way, the average temperature for the upper 100m of water at 1800 GMT, 23 September 1975 is found to be 23.849°C. Using this information and equation (3a) finite differenced about 1500 GMT, 23 September 1975, the change in heat content of the 100m column is calculated as

$$(\frac{\Delta H}{\Delta t})_{1500GMT} = \rho C_p z (\frac{\Delta T}{\Delta t})_{1200-1800GMT}$$

$$= \frac{1gm}{cm^3} \cdot \frac{1cal}{gm\text{-}°C} \cdot 10000cm \frac{(23.849-23.501)°C}{6\ hr} = 580cal/cm^2/hr$$

25

The surface flux term calculated from equation (4) was 45 cal/cm^2/hr. The only remaining variables needed to solve for the mass transport at 100m are $(T_{av})_{0--100m}$ and T_B for 1500 GMT. These are available from, respectively, equation (11) and the regression curve computed for 1500 GMT and are equal to 23.378 and 19.072°C. Since M_{z_T} is assumed to be zero at the ocean surface, equation (10) can now be solved for M_{z_B}:

$$M_{z_B} = \frac{-580 - 45}{23.378 - 19.072}$$

$$= -146 \text{ gm/}cm^2\text{/hr, which, for the column one}$$

square centimeter in cross-section corresponds, since ρ was fixed at a value of one in equation (10a), to a downward velocity of 1.46m/hr. This is the downward velocity necessary to advect the heat to produce the change observed in the logarithmic temperature profiles. For the mass transport values at the 200m and all deeper levels, the value of Q_n in equation (10) is zero. The value for M_{z_T} in the 100--200m layer is simply the value of M_{z_B} in the 0--100m layer immediately above and the T_{av} is obtained from equation (13). The right-hand set of arrows in Figure 4 shows the values of vertical velocity calculated using equation (10a) at each level for the observation time under consideration.

In summary, the vertical velocities at levels of 100m increments were calculated for 1500 GMT 23 September 1975 two ways, first using equation (5a) and then using equation (10a).

Only the right-hand set of values in Figure 4 satisfies the heat budget, and may be compared with the left-hand set to estimate the effect of omitting the horizontal heat flux as in equation (5a). A similar set of calculations, using both the equation (5a) method and the

26

equation (10a) method was made for each of the 55 observation times from
1300 GMT, 20 September to 1200 GMT, 26 September 1975, which is when the
meteorological sensors on the buoy were turned off. Due to the finite
differencing scheme in time, this period was expanded, for averaging
purposes, to 1230 GMT, 20 September to 1330 GMT, 26 September 1975--a
span of 145 hr.

III. RESULTS

A. RESULTS OF THE MIXED LAYER DEPTH STUDY

Table 1 is a list of the estimated values of MLD versus time for
the period 1200 GMT, 20 September to 1200 GMT, 26 September 1975. The
column in Table 1 headed DTG gives the day of September by the first
two digits and the GMT hour by the last two digits. Figure 5 shows the
same variables graphically for the period 1200 GMT, 20 September 1975
to 1200 GMT, 11 October 1975. The ordinate in Figure 5 is positioned
at the time of passage of Eloise over EB-10--0300 GMT, 23 September 1975.
Notice that according to this graph, the average depth of the mixed
layer was roughly 33 meters prior to storm approach and deepened grad-
ually as the hurricane winds increased. An upwelling of the thermocline,
i.e. a decreasing of mixed layer depth began at the time of hurricane
passage. At 1500 GMT, 23 September 1975, or about 12 hr after eye
passage, the MLD reached a minimum of 21.98m as calculated from the re-
gression temperature profile for this observation time. Following that
time the MLD swung through at least three distinct oscillations with
nearly perfect inertial cycle periodicity (the inertial period at the
latitude of EB-10 is 26.0 hr). These oscillations are superposed on a
continued deepening trend before finding an equilibrium vacillation

with a combined inertial-diurnal period centered around a depth of about 52m. Thus the net mixed layer deepening due to storm passage was about 19m. Notice in Figure 6 the amplitude of the first three wave peaks following passage of the eye of the storm over EB-10. All three of these oscillations of the thermocline are significantly larger in amplitude than those either before or after the storm. If the average amplitude of the post-storm oscillations is subtracted from the amplitude of the three largest, the amplitude of each successive oscillation decreases by roughly e^{-1} of the prior value. Also, as shown in Figure 6, if an approximation of the zero crossing is drawn through the oscillations, a rough curve of e^{-kt} is produced. The rate of dampening of these large oscillations is important for predicting the duration of the storm wake and for verification of numerical models.

B. RESULTS OF THE ISOTHERM POSITION STUDY

Figure 7 is a graph of seven isotherms within the thermocline during the three days before and 18 days after Hurricane Eloise passed. In comparing this graph with Figure 1--NDBO's version assuming linear temperature gradients--it can be seen that overall, the general trend of the upper isotherms is the same, each graph having three distinct oscillations followed by a net deepening after hurricane passage. One notes in Figure 7 that the isotherm depths are relatively uniform prior to hurricane passage. The first three upwelling cycles are distinct and nearly uniform throughout the upper thermocline. Following this period the oscillations are much smaller in the upper thermocline, in agreement with the estimated mixed layer depths in Figure 5. However, the oscillations continue with considerable amplitude at greater depths. It is important to note that over the entire period the mean depth of

DTG	MLD(m)		DTG	MLD(m)
2012	31.03		2309	36.44
2013	33.26		2312	22.47
2015	33.68		2315	21.98
2018	30.12		2318	26.39
2021	31.74		2400	41.90
2100	34.14		2403	49.31
2103	33.27		2406	50.14
2106	33.59		2409	48.90
2109	32.95		2412	43.83
2112	31.70		2415	35.05
2115	33.75		2418	35.41
2118	33.05		2421	40.42
2121	33.41		2500	44.91
2200	34.27		2503	52.02
2203	34.20		2506	53.67
2206	37.55		2507	53.74
2209	35.60		2508	53.56
2212	36.60		2509	53.16
2215	35.47		2510	52.30
2218	35.29		2511	51.20
2221	35.77		2512	50.12
2222	35.35		2515	46.20
2223	37.16		2518	39.53
2300	38.47		2521	42.24
2301	39.31		2600	43.37
2303	41.85		2603	46.92
2306	39.08		2609	54.04
			2612	53.34

TABLE 1. Depth of mixed layer with time. Left-hand column gives the day of September by the first two digits and the GMT hour by the last two digits. Values of mixed layer depth in the right-hand column were found by entering the respective regression equation with the surface temperature to get the pressure at the bottom of the mixed layer, and then converting from pressure to depth in meters.
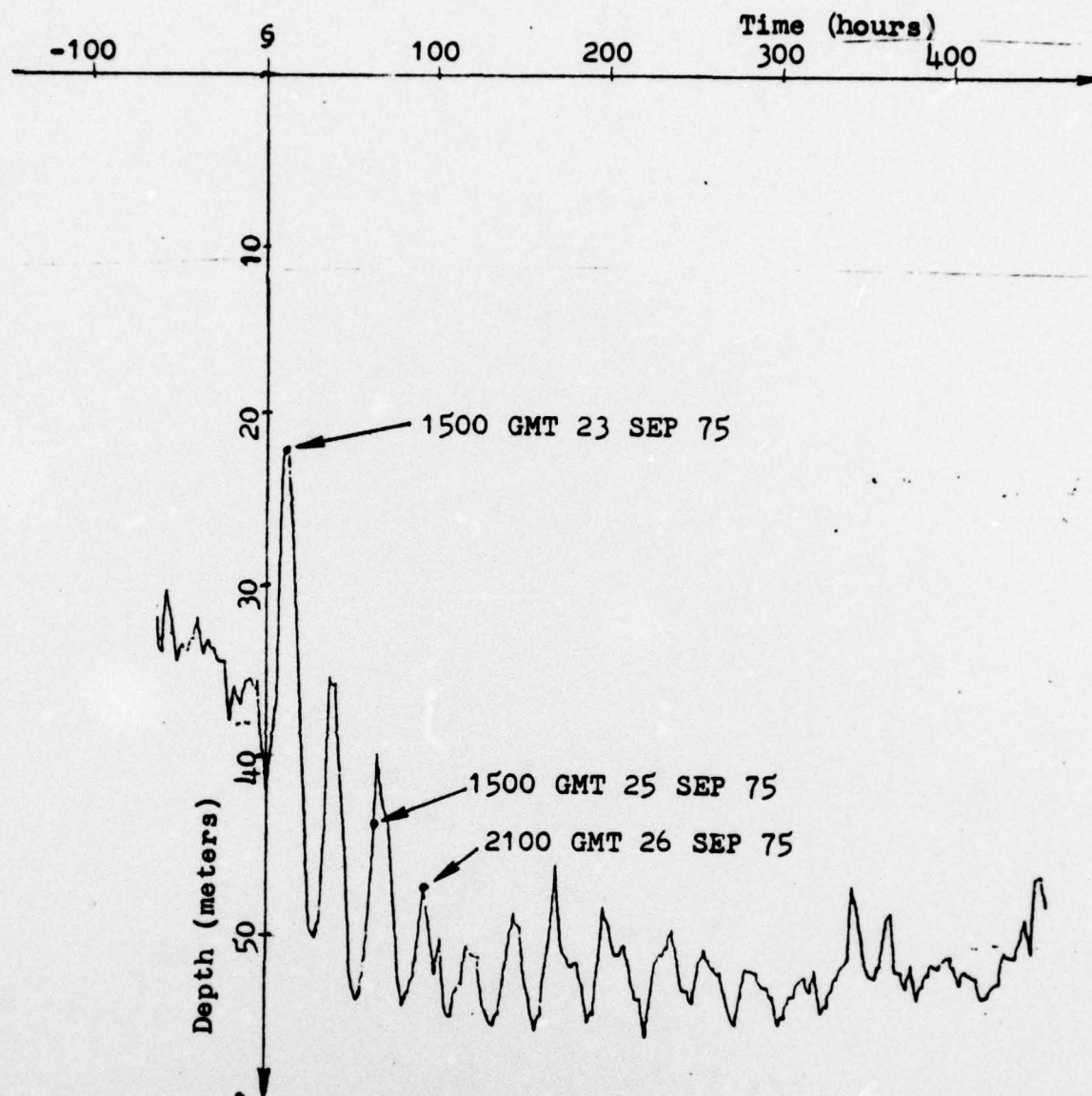
FIGURE 5. Graph of mixed layer depth vs. time. Ordinate shows depth in meters and is positioned along x-axis at time of hurricane passage. The average mixed layer depth was roughly 33m prior to storm approach. At hurricane passage a 12hr period of upwelling began, followed by three distinct oscillations of the thermocline. Average depth of the mixed layer after these three distinct oscillations was roughly 52m.
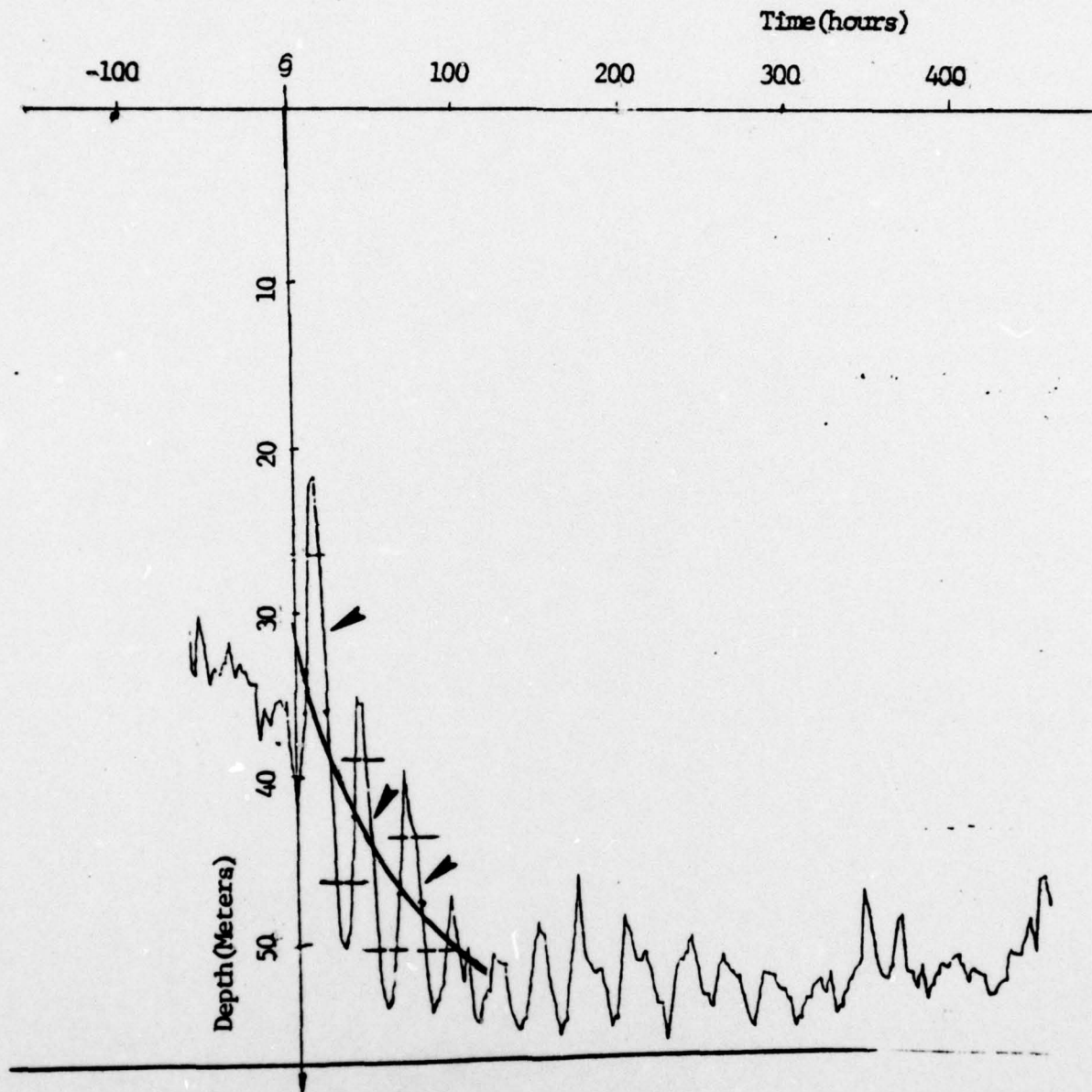
FIGURE 6. Decay of internal wave amplitude and mixed layer deepening rate. A rough approximation of the average post-storm amplitude of thermocline oscillation was subtracted from the amplitude of the three distinct oscillations immediately after hurricane passage. The remaining length of the downward strokes, indicated by the three arrows, was then measured. The values were found to decrease by roughly e^{-1} of the former value. Also a rough approximation of the zero crossing (heavy black line) suggests that the rate of deepening of the mixed layer is e^{-kt}.

31
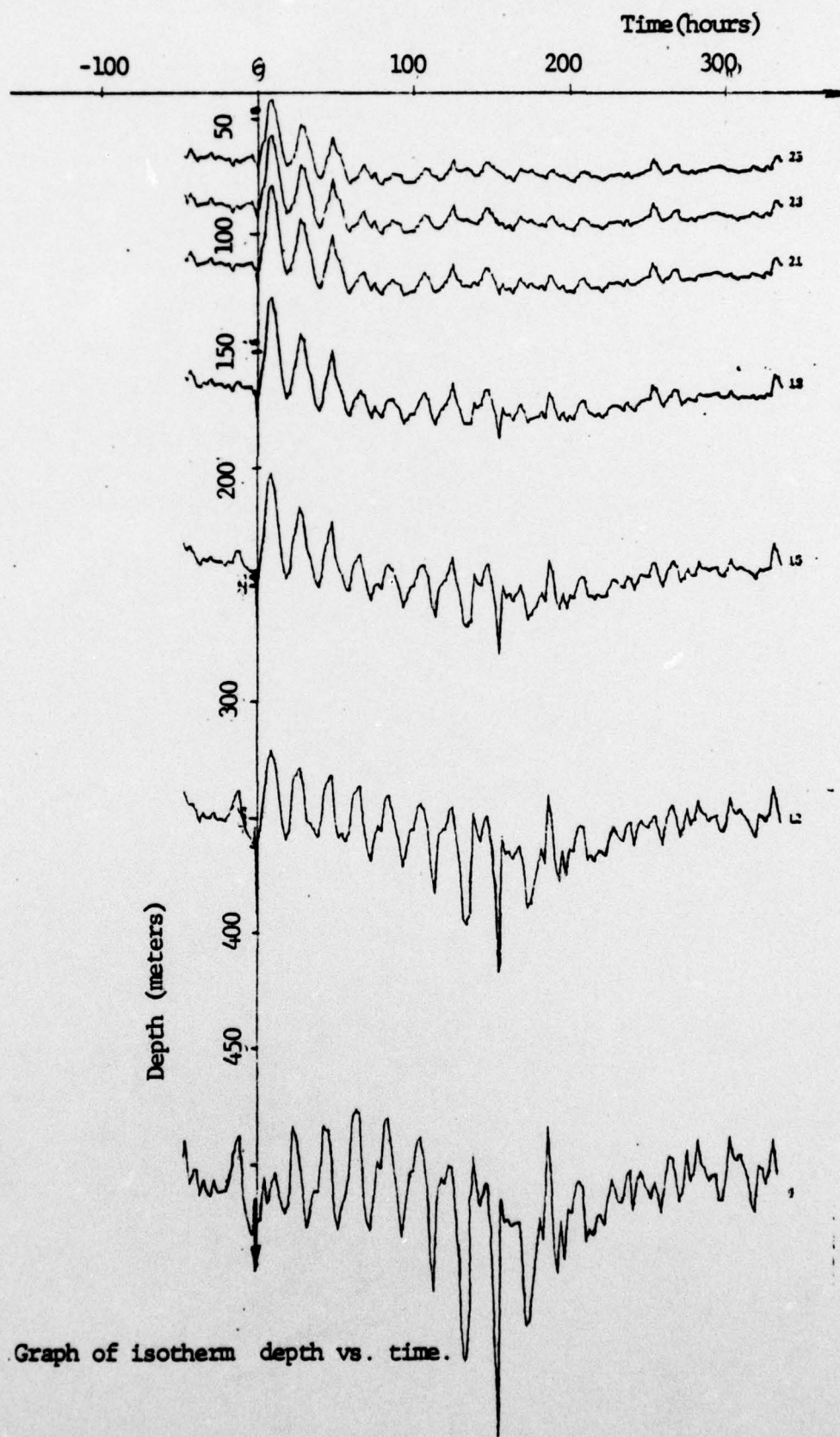
FIGURE 7. Graph of isotherm depth vs. time.

each isotherm does not change significantly, which is equivalent to stating that the mean temperature in the column does not change significantly. Nevertheless, there is a net depression of the isotherms for about 10 days following hurricane passage. In this period there must be a net downward vertical motion. Further investigation of these isotherms and the meaning of their changing position in time applies to the problem of balancing the heat budget, the results of which are discussed next.

C. RESULTS OF THE HEAT BUDGET STUDY

Figure 8 shows the calculated logarithmic temperature profiles for a pre-storm (solid line) and a typical post-storm (dashed line) observation time down to the 200m level. As expected, there was a cooling and deepening of the mixed layer. The warming of the water column below the mixed layer supports the net isotherm lowering observable in Figure 7 and is suggestive of heat transport by downward vertical velocities. It was desired to solve the heat budget to calculate these vertical velocities. But an oscillating thermocline requires averaging vertical velocity over an integer number of cycles, otherwise the heat budget is obscured by apparent heat storage. Hence it was decided to solve the heat budget in four parts (see Figure 9), the first part being the nearly three-day period of storm approach, the second part being the period of tremendous upwelling from the time of hurricane passage until 1330 GMT, 23 September, the third part being the period from 1330 GMT, 23 September to 1630 GMT, 25 September (a 51hr period at a latitude where inertial cycles are 26.0hr, chosen because of the distinctiveness of the periodicity), and the fourth part being the period from 1630 GMT, 25 September until 1330 GMT, 26 September--one and one-half hours after
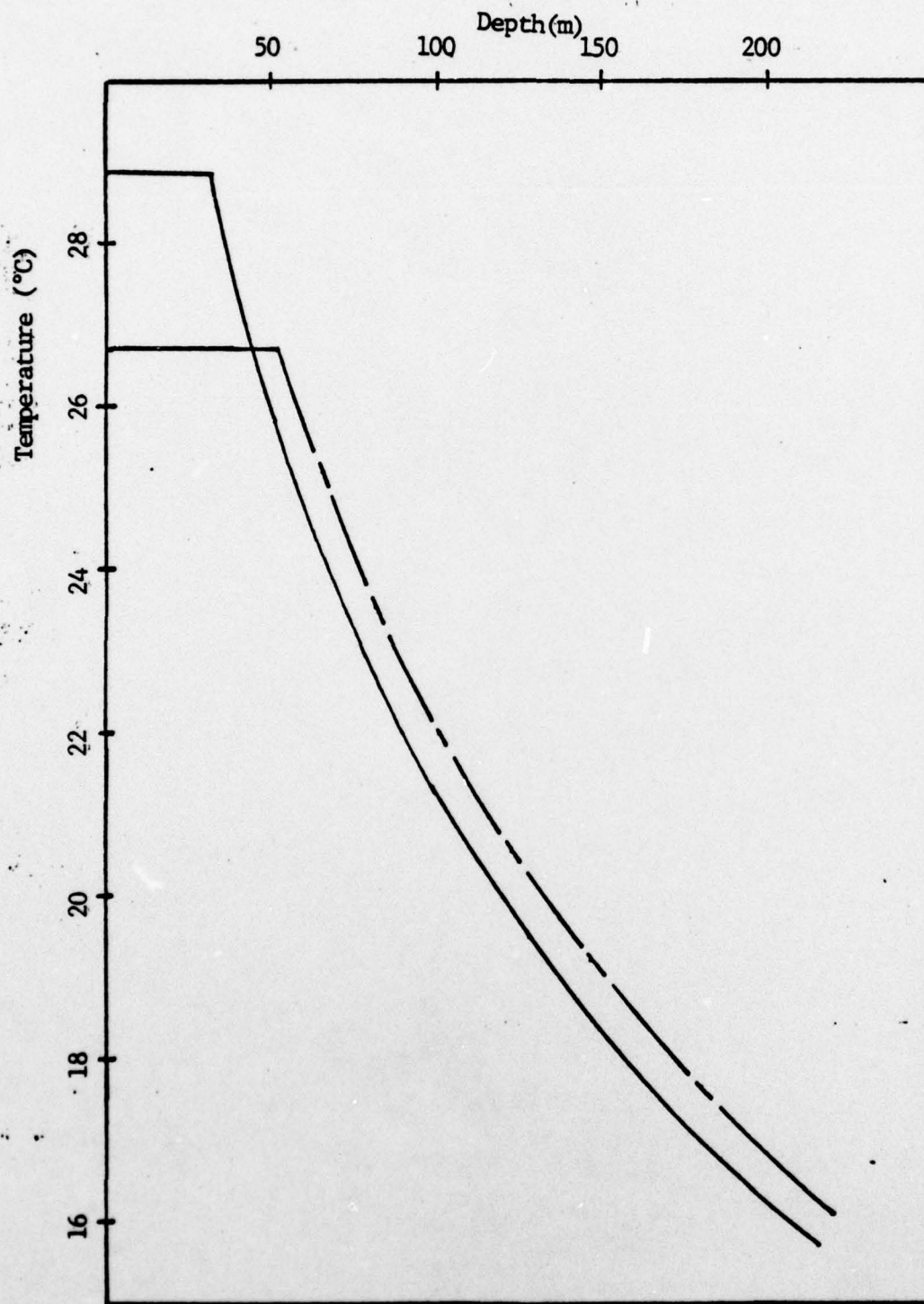
FIGURE 8. Graph of temperature vs. depth for typical pre-storm (solid line) and post-storm (dashed line) observation times. MLD deepened from roughly 33m to 52m while cooling more than 2°C. Notice isotherm lowering.
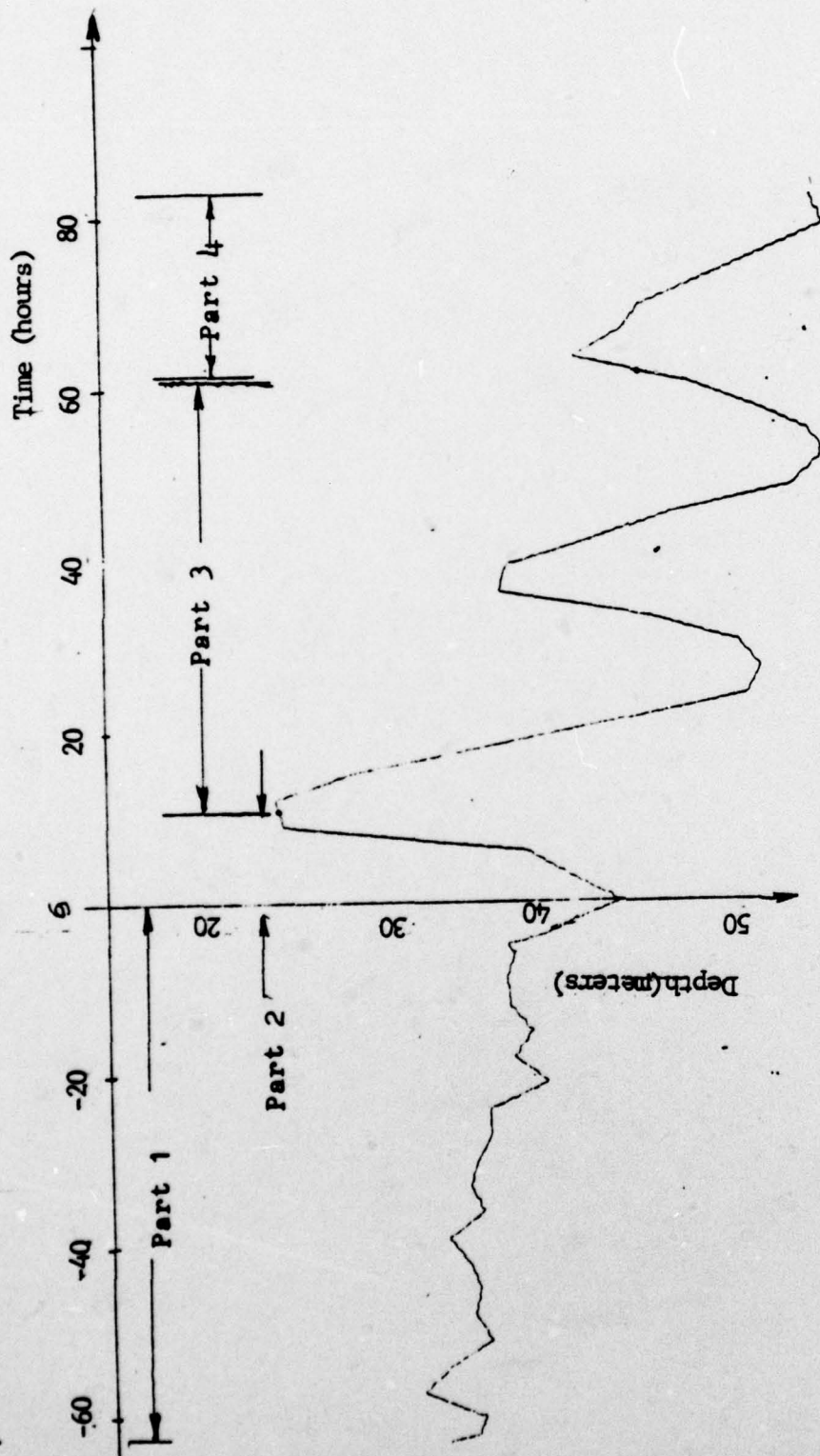
FIGURE 9. Time spans of the four parts of the heat budget. This graph is an expansion of the MLD estimates of FIGURE 5, and shows the period of storm approach (Part 1), the period of intense upwelling immediately after hurricane passage (Part 2), two large-scale cycles of thermocline oscillations (Part 3) and the remainder of the time during which the meteorological sensors were turned on (Part 4).

35

the meteorological sensors on the buoy were turned off. The total length of averaging time was 145hr. Vertical velocities for each of the 55 observation times during this 145hr period were calculated two ways, using equation (5a), and using equation (10a). Table 2 shows the values obtained through equation (5a) under the columns headed w and the values obtained through equation (10a) under the columns headed $M_{z/\rho}$. The values are given for five depths for all 55 observation times considered. The mean values for each of the four parts of the heat budget were calculated by weighting each value with the appropriate time interval in the far-right column, which is one-half of the time span between the previous and the subsequent observations.

Figure 10 shows schematically the mean values over the entire period listed in Table 2 for the five levels considered. The corresponding horizontal mass transports were obtained using equation (8). Individual values of w vs. $M_{z/\rho}$ at all depths in Table 2 together with the information supplied by Figure 10 illustrate the following points regarding the four parts of the heat budget.

1. Part One

During this period the vertical velocities deduced by both methods are generally similar in sign and magnitude. Larger vertical motions are found by both methods during the 24 hours prior to the end of the period (time of hurricane passage), particularly at lower levels. These values are several times the mean values over the period, which are generally downward.

2. Part Two

This period was selected to illustrate the rapid upwelling just after hurricane passage. Average values of 5m/hr for this 12-hour

period are not uncommon. The w values from equation (5a) without
horizontal temperature advection effects included have a more uniform
vertical profile (left side of Figure 10, Part 2) than those calculated
from equation (10a). However, as noted before, the values on the left
side of Figure 10 do not satisfy the heat budget.

3. Part Three

During this period the thermocline region is oscillating from
its highest upward excursion. It may be noted in Table 2 Part 3 that
the positive and negative vertical motions are not in phase after about
0300 GMT, 24 September 1975. As indicated in Figure 10 Part 3, the
lower level mean vertical motion becomes upward at 500m whereas the
levels nearer the surface are still experiencing downward vertical motion.

4. Part Four

This portion of the record contains the third oscillation of the
thermocline following the hurricane passage. It appears that the ver-
tical motion oscillation at 100m is about 90 degrees out of phase with
that at 500m by 0900 GMT, 26 September 1975. Rather large mean verti-
cal motion values (Figure 10 Part 4) are shown at several levels be-
cause not a complete inertial cycle is included in the period. The
vertical structure of alternating inflow and outflow with depth on the
right side of Figure 10 Part 4 contrasts with the more uniformly
varying inflow/outflow vertical structure deduced from vertical motion
as calculated via equation (5a).

D. ERROR DISCUSSION

According to Withee and Johnson [1976], the data were accurate to
within $0.1 kg/cm^2$ in pressure, representing about one meter in depth, and

DTG	w_{100}	M_{100}/ρ	w_{200}	M_{200}/ρ	w_{300}	M_{300}/ρ	w_{400}	M_{400}/ρ	w_{500}	M_{500}/ρ	weight
2013	-1.26	-1.72	-1.24	-0.78	-0.79	-1.36	-0.05	0.55	0.09	0.25	1.5
2015	0.70	1.31	0.11	-0.53	-0.93	-0.12	-2.27	-3.11	-3.83	-2.89	2.5
2018	0.30	0.37	0.08	0.03	-0.32	-0.23	-0.83	-0.92	-1.44	-1.35	3
2021	-1.08	-1.52	-1.02	-0.56	-0.57	-1.16	0.12	0.73	1.00	0.31	3
2100	-0.47	-0.50	-0.83	-0.79	-1.17	-1.22	-1.50	-1.44	-1.81	-1.86	3
2103	0.23	0.43	0.14	-0.07	-0.06	0.22	-0.34	-0.62	-0.67	-0.34	3
2106	0.14	0.15	0.20	0.18	0.25	0.26	0.28	0.25	0.30	0.32	3
2109	0.36	0.48	0.19	0.08	-0.17	-0.04	-0.65	-0.78	-1.22	-1.07	3
2112	-0.16	-0.32	-0.02	0.17	0.23	0.02	0.54	0.76	0.90	0.67	3
2115	-0.34	-0.48	-0.34	-0.20	-0.24	-0.42	-0.06	0.14	0.18	-0.03	3
2118	0.09	0.28	-0.06	-0.28	-0.30	-0.05	-0.59	-0.86	-0.92	-0.65	3
2121	-0.22	-0.29	-0.21	-0.14	-0.12	-0.22	0.01	0.10	0.19	0.07	3
2200	-0.12	-0.24	-0.01	0.12	0.17	0.02	0.42	0.58	0.70	0.53	3
2203	-0.43	-0.51	-0.05	-0.01	0.61	0.53	1.45	1.51	2.43	2.35	3
2206	0.03	-0.03	0.51	0.54	1.15	1.08	1.90	1.97	2.74	2.64	3
2209	0.39	0.37	0.73	0.75	1.06	1.02	1.39	1.43	1.72	1.67	3
2212	-0.09	0.13	-0.68	-0.91	-1.45	-1.16	-2.35	-2.66	-3.34	-3.00	3
2215	0.17	0.68	-0.79	-1.32	-2.16	-1.48	-3.79	-4.49	-5.63	-4.87	3
2218	0.17	0.71	-0.24	-0.87	-0.86	-0.13	-1.62	-2.41	-2.48	-1.63	3
2221	0.25	0.76	-0.10	-0.68	-0.67	0.02	-1.37	-2.10	-2.18	-1.37	2
2222	-0.52	-0.08	-0.89	-1.46	-1.22	-0.59	-1.53	-2.24	-1.81	-1.07	1
2223	-1.73	-1.96	-1.71	-1.55	-1.11	-1.37	-0.12	0.12	1.15	0.90	1
2300	-0.68	-1.11	0.53	0.90	2.40	1.90	4.72	5.25	7.37	6.80	1
2301	-2.01	-1.27	-6.17	-1.09	-11.18	-0.91	-16.75	-0.09	-22.74	0.48	1.5
Mean	-0.14	-0.06	-0.33	-0.28	-0.54	-0.20	-0.77	-0.46	-1.01	-0.34	

TABLE 2. Vertical velocities for each observation time and mean values (four-part heat budget). Part 1 is on this page and Parts 2,3, and 4 are on the next three pages. For each depth, the values of w were obtained using equation (5a), while the values of M_z/ρ were obtained using equation (10a). The mean values were calculated by weighting each velocity by the figure in the far-right column, which is one-half the time span between the previous and the subsequent obser- vations. All values have units of m/hr.

DTG	w_{100}	M_{100}/ρ	w_{200}	M_{200}/ρ	w_{300}	M_{300}/ρ	w_{400}	M_{400}/ρ	w_{500}	M_{500}/ρ	weight
2303	2.62	3.16	4.99	-1.13	7.34	3.10	9.70	-3.25	12.05	1.44	2.5
2306	2.92	4.73	3.80	1.71	4.05	6.52	3.87	1.52	3.37	5.94	3
2309	4.48	6.32	5.18	3.18	4.65	7.09	3.31	0.75	1.36	4.21	3
2312	4.16	5.07	4.45	3.63	3.46	4.60	1.63	0.55	-0.83	0.46	3
Mean	3.58	4.89	4.59	1.98	4.77	5.35	4.41	0.03	3.64	3.08	

TABLE 2, Part 2.

DTG	w_{100}	M_{100}/ρ	w_{200}	M_{200}/ρ	w_{300}	M_{300}/ρ	w_{400}	M_{400}/ρ	w_{500}	M_{500}/ρ	weight
2315	-0.91	-1.46	-0.61	-0.03	0.11	-0.61	1.10	1.86	2.30	1.45	3
2318	-3.77	-4.61	-4.33	-3.54	-3.84	-4.89	-2.67	-1.63	-0.97	-2.16	4.5
2400	-3.36	-4.16	-4.05	-3.27	-3.87	-4.88	-3.13	-2.10	-1.95	-3.11	4.5
2403	-0.89	0.07	-1.00	-2.25	-0.86	0.52	-0.54	-2.09	-0.10	1.55	3
2406	1.03	1.72	2.27	1.39	3.63	4.62	5.06	3.97	6.55	7.70	3
2409	1.91	2.48	2.94	2.28	3.71	4.49	4.31	3.48	4.79	5.72	3
2412	2.87	3.67	2.64	1.90	1.37	2.35	-0.59	-1.57	-3.06	-1.92	3
2415	1.52	1.78	0.95	0.79	-0.34	-0.07	-2.10	-2.32	-4.22	-3.93	3
2418	-1.83	-2.04	-2.85	-2.64	-3.65	-3.93	-4.29	-4.01	-4.82	-5.16	3
2421	-2.36	-2.82	-2.91	-2.36	-2.88	-3.58	-2.47	-1.76	-1.76	-2.59	3
2500	-2.51	-3.25	-2.35	-1.60	-1.29	-2.27	0.36	1.36	2.45	1.31	3
2503	-2.20	-3.59	-2.21	-0.66	-1.48	-3.34	-0.27	1.70	1.31	-0.86	2
2506	-1.17	-2.56	-1.23	0.33	-0.92	-2.74	-0.36	1.61	0.37	-1.78	1
2507	-0.14	-1.19	0.65	1.88	1.78	0.33	3.12	4.68	4.64	2.93	1
2508	0.82	1.03	1.69	1.40	2.62	2.95	3.58	3.21	4.56	4.95	1
2509	1.74	2.87	2.74	1.37	3.54	5.13	4.20	2.47	4.75	6.62	1
2510	2.40	3.41	4.22	3.83	5.89	6.34	7.47	6.98	8.99	9.55	1
2511	2.31	3.42	3.39	2.10	4.08	5.60	4.53	2.90	4.80	6.59	1
2512	1.94	2.86	1.99	0.99	1.41	2.65	0.43	-0.88	-0.87	0.58	2
2515	2.28	3.04	2.16	1.42	1.22	2.17	-0.25	-1.22	-2.11	-1.01	3
Mean	-0.52	-0.60	-0.55	-0.45	-0.34	-0.45	-0.04	0.06	0.34	0.22	

TABLE 2 Part 3

40

| DTG	w_{100}	M_{100}/ρ	w_{200}	M_{200}/ρ	w_{300}	M_{300}/ρ	w_{400}	M_{400}/ρ	w_{500}	$M_{500}\rho$	weight
2518	-0.07	-0.42	-1.10	-0.58	-2.49	-3.05	-4.10	-3.47	-5.89	-6.57	3
2521	-1.83	-2.02	-3.00	-2.81	-3.98	-4.22	-4.84	-4.60	-5.61	-5.91	3
2600	-1.23	-1.79	-1.37	-0.77	-1.16	-1.89	-0.71	+0.05	-0.07	-0.93	3
2603	-1.99	-2.92	-1.83	-0.83	-0.95	-2.19	0.40	1.69	2.10	0.67	3
2606	-1.49	-2.16	-1.27	-0.56	-0.48	-1.35	0.69	1.62	2.15	1.14	3
2609	0.07	-0.11	1.09	1.23	2.46	2.25	4.05	4.24	5.82	5.59	3
2612	0.66	0.56	1.60	1.68	2.67	2.56	3.82	3.91	5.03	4.92	3
Mean	-0.84	-1.27	-0.84	-0.38	-0.56	-1.13	-0.10	0.49	0.50	-0.16	

TABLE 2   Part 4

41
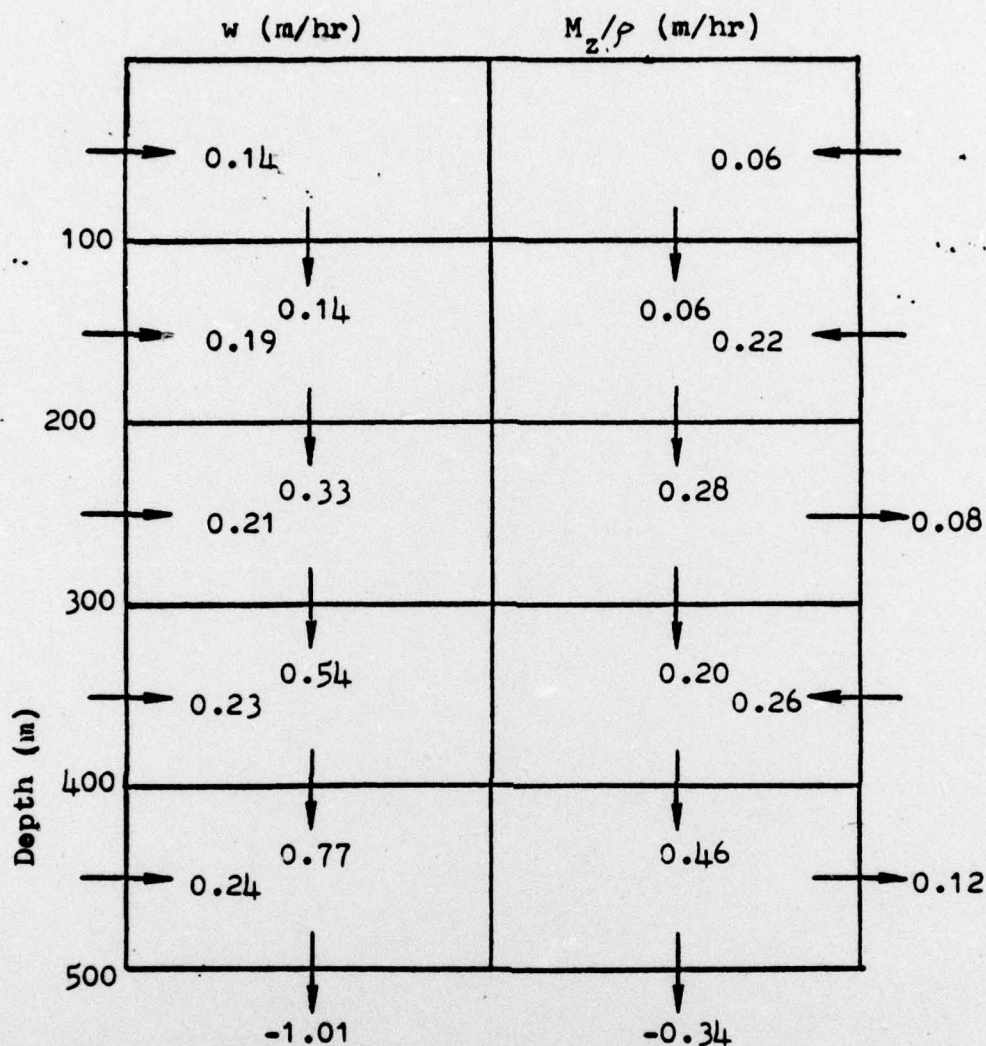
FIGURE 10. Mean values of vertical velocities at five depths (four-part heat budget). Part 1 is on this page and Parts 2, 3 and 4 are on the next three pages. Values of w in left column were obtained using equation (5a), i.e. assuming zero horizontal temperature advection. Values of M_z/ρ in right column were obtained using equation (10a), i.e. not assuming zero horizontal temperature advection. The corresponding values of horizontal mass transport were obtained using equation (8), represent the total mass transport across all vertical faces of the column, and have the units of hectograms per hour.
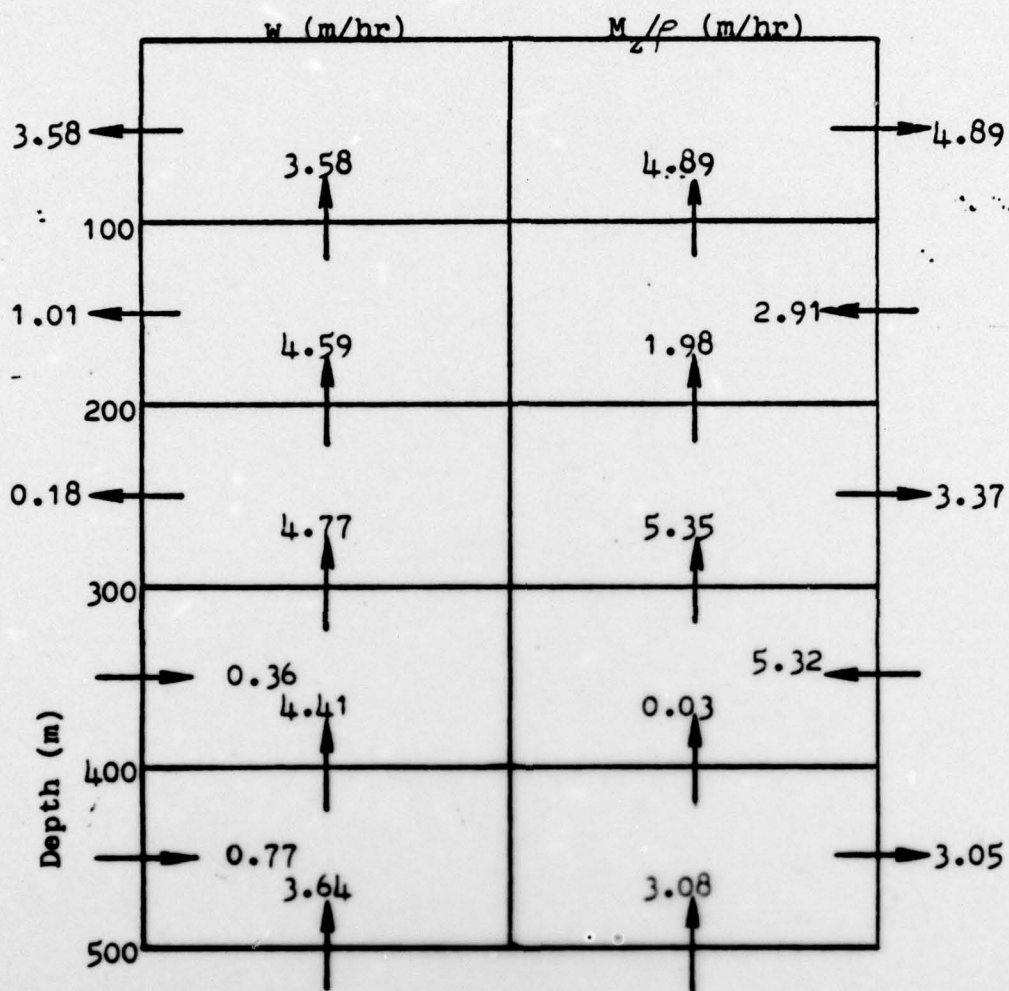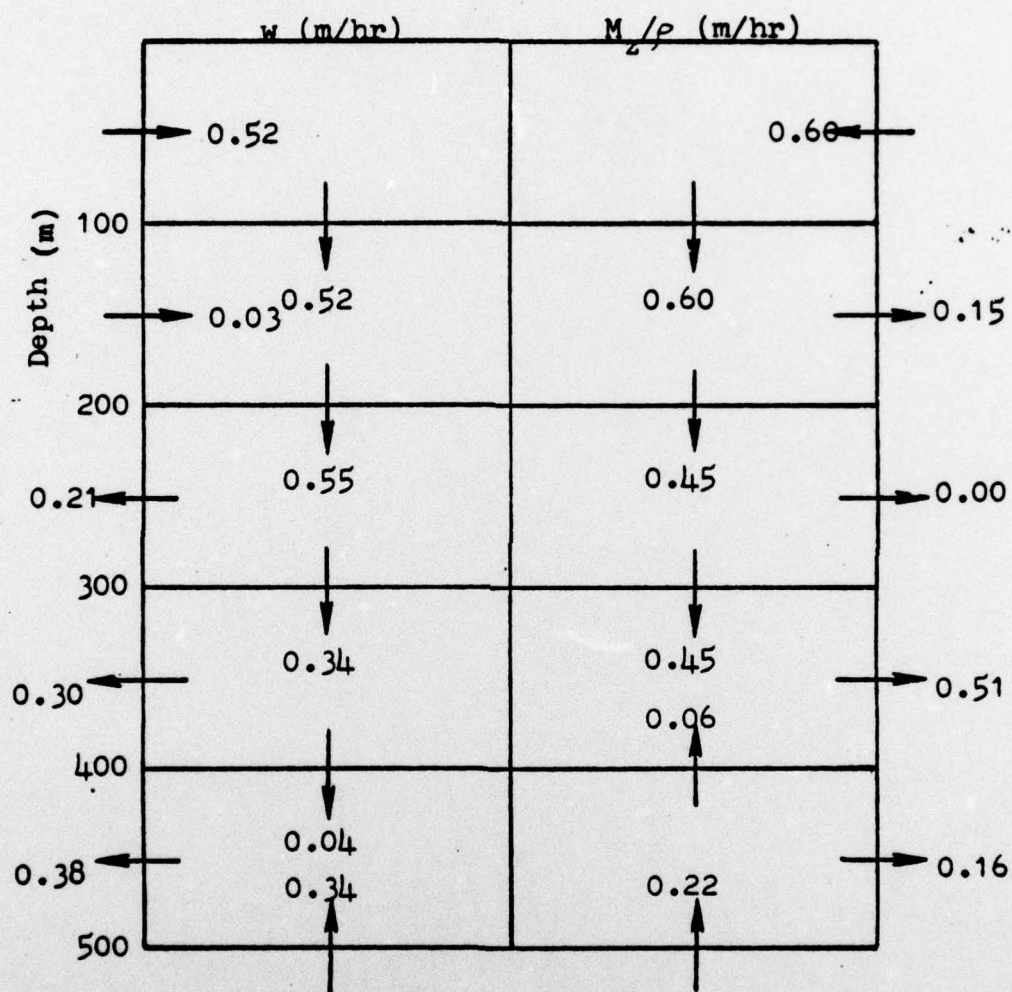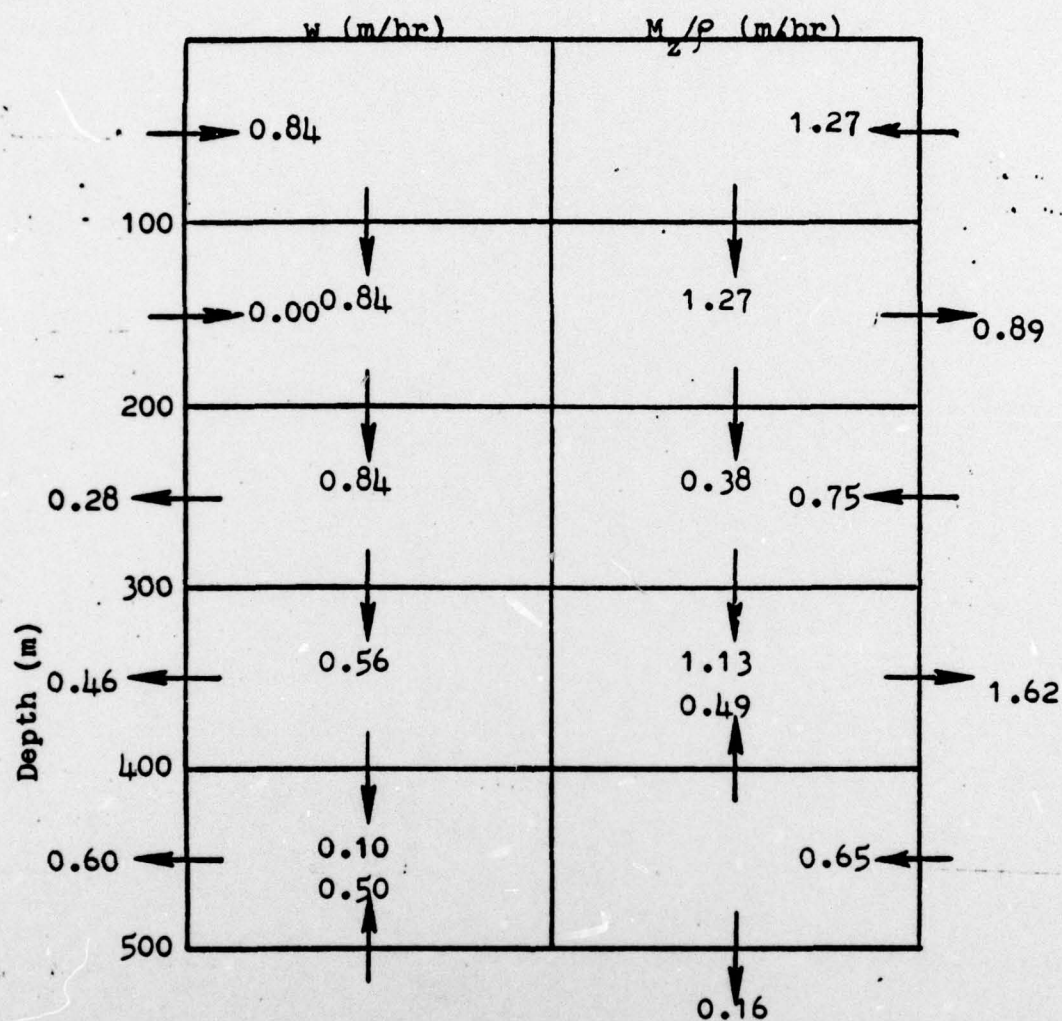
FIGURE 10   Part 2

43

FIGURE 10, Part 3

44

FIGURE 10, Part 4

±0.05°C in temperature except near the top of the thermocline where the accuracy dropped to ±0.20°C. Ideally then, the errors induced by the regression temperature profiles should fall within these tolerances. Table 3 shows the observed and regression temperatures and the error for each of the times used in Parts 2,3 and 4 of the heat budget calculation, all of which were more erroneous than part 1. Since the columns headed T_{50}, T_{200} and T_{500} are the temperatures observed by the three subsurface sensors on EB-10, it is emphasixed that these measurements were made as the sensors migrated above and below these nominal depths in response to buoy movement.

The root mean square regression temperature error for the three columns are shown in Table 3. Note that at 50m the temperature ranges from about 23°C to 26.7°C, the largest error in fitting the profile is about 0.25°C. Whereas the error values are somewhat outside the expected accuracy of the instruments, it should be noted that the storage term in equation (10) depends more on the temperature gradient than on the absolute value of temperature. The smooth variation in time of the temperature profiles derived by this method were important for the heat budget calculations.

The accuracy of calculating the MLD using the logarithmic temperature profiles deserves comment. Of course the accuracy of the MLD is limited by the accuracy of each regression curve. Given an accurate regression curve and a surface temperature accurate to within ±0.20°C, the MLD as calculated in this thesis would be known to within ±2m. The accuracy of the MLD is certainly governed by the accuracy of the method, i.e., the very idea of calculating the MLD assuming an isothermal mixed layer above a logarithmic temperature profile. This model has not been used in the past.

DTG	$(T_r)_{500}$	ERR_{50}	$(T_r)_{200}$	ERR_{200}	$(T_r)_{500}$	ERR_{500}
2303	26.727	-0.118	16.462	0.324	9.810	-0.205
2306	26.916	-0.109	17.159	0.291	11.027	-0.182
2309	25.887	0.033	16.417	-0.080	10.094	0.047
2312	23.334	0.164	15.009	-0.376	9.547	0.211
2315	22.936	0.247	14.612	-0.543	9.171	0.296
2318	23.332	0.193	14.586	0.439	8.860	-0.245
2400	25.549	-0.124	15.788	0.342	9.348	-0.217
2403	26.290	-0.085	16.282	0.225	9.696	-0.141
2406	26.181	-0.023	16.216	0.058	9.600	-0.035
2409	25.776	-0.088	15.268	0.232	8.309	-0.144
2412	25.160	0.017	15.071	-0.044	8.400	0.026
2415	24.143	0.152	14.842	-0.353	8.705	0.200
2418	24.137	0.036	14.936	-0.089	8.888	0.053
2421	24.799	0.057	15.336	-0.139	9.157	0.082
2500	25.294	-0.008	15.487	0.021	9.072	-0.013
2503	26.240	-0.084	15.821	0.224	8.968	-0.139
2506	26.647	-0.078	16.052	0.205	9.048	-0.127
2507	26.736	-0.059	15.961	0.154	8.850	-0.095
2508	26.731	-0.054	15.778	0.141	8.568	-0.086
2509	26.618	-0.078	15.622	0.206	8.426	-0.128
2510	26.483	-0.101	15.538	0.272	8.323	-0.170
2511	26.363	-0.112	15.505	0.299	8.276	-0.187
2512	26.155	-0.119	15.466	0.320	8.343	-0.201
2515	25.555	-0.098	15.267	0.261	8.431	-0.163
2518	24.672	-0.039	15.007	0.102	8.682	-0.063
2521	25.295	-0.097	15.389	0.263	8.920	-0.165
2600	25.450	-0.044	15.540	0.114	9.065	-0.070
2603	25.943	-0.070	15.660	0.184	8.890	-0.114
2606	26.647	-0.038	15.807	0.100	8.753	-0.061
2609	26.986	-0.061	15.807	0.160	8.526	-0.098
2612	26.828	-0.137	15.424	0.378	7.983	-0.240
RMS		0.102		0.255		0.153

TABLE 3. Error in regression temperatures as compared to observed temperatures. Error (ERR) is defined as regression temperature (T_r) minus observed temperature (T). Both T_r and T are for sensor depth (which varied), although the nominal depths of 50, 200 and 500m were used in naming these variables. Root-mean-square of the three columns of errors is given.

IV. SUMMARY AND CONCLUSIONS

The buoy EB-10 measured the temperature at the surface and three time-varying subsurface depths during the passage of Hurricane Eloise. In order to study mixed layer deepening, thermocline response and the heat budget, temperature profiles were needed that represented the thermal structure of the ocean from surface to depth following storm passage. These profiles were calculated assuming an isothermal mixed layer above a thermocline with temperature proportional to the natural logarithm of hydrostatic pressure. The resulting graph of mixed layer depth (MLD) versus time showed that prior to the arrival of Eloise at EB-10, the average mixed layer depth was about 33m. As the winds increased due to hurricane approach, the mixed layer deepened steadily to about 42m before upwelling to approximately 22m. The thermocline then underwent three distinctly large oscillations of inertial periodicity, while the mixed layer continued to deepen. The post-storm average mixed layer depth was about 52 meters.

Vertical velocities, calculated first by assuming zero horizontal temperature advection in the material derivative equation and second by finding the mass transport necessary to balance the heat budget, show that in the upper 500m of the water column downward vertical motion of 1m/hr or less prevailed during storm appraoch, followed by upward vertical velocity as great as 5.35m/hr during the 12 hours immediately following hurricane passage. Next, during a 51-hour period in which the thermocline underwent the first two of three large oscillations, downward vertical velocity on the order of 0.5m/hr prevailed in the upper 300m of the water column with slight upward velocity at the 400m and 500m levels.

The heat budget could not be solved during the entire period of the third
large oscillation of the thermocline because the meteorological sensors
on the buoy had been shut off, but during the first half of the third
oscillation, i.e., the downward stroke, calculated vertical velocity was
generally downward, as great as 1.27m/hr.

Although the time-averaged values of vertical velocities obtained by
neglecting horizontal temperature advection were generally in good agree-
ment with those obtained considering horizontal temperature advection in
all four parts of the heat budget study, when comparing the individual
values comprising the averages of the two methods, one sees that the mag-
nitudes of the velocities differ significantly. The values obtained by
considering horizontal advection are assumed to be more accurate.

LIST OF REFERENCES

1. Black, P.G., and Mallinger, W.D., 1972: The Mutual Interaction of Hurricane Ginger and the Upper Mixed Layer of the Ocean. 1971 Project Stormfury Annual Report, Dept. of Commerce, 63-87.

2. Black, P.G., and Withee, G., 1976: The Effect of Hurricane Eloise on the Gulf of Mexico (abstract). Bull. Amer. Meteor. Society, 57, p 139.

3. Denman, K.L., and Miyake, M., 1973: A Time- Dependent Model of the Upper Ocean, J. Phys. Oceanogr., 3, pp. 185-196.

4. Elsberry, R.L., Fraim, T.S., and Trapnell, R.N., 1976: A Mixed-Layer Model of the Oceanic Thermal Response to Hurricanes, Journal of Geophysical Research, 81, pp. 1153-1162.

5. Elsberry, R.L., Pearson, N.A.S., and Corgnati, L.B., Jr., 1974: A Quasi-Empirical Model of the Hurricane Boundary Layer, Journal of Geophysical Research, 79, pp. 3033-3040.

6. Fedorov, K.N., 1973: The Effect of Hurricanes and Typhoons on the Upper Active Ocean Layers, Oceanology, 12, pp. 329-332.

7. Fraim, T.S., 1973: Oceanic Thermal Response to a Time-Dependent Hurricane Model, M.S. Thesis, Naval Postgraduate School, Monterey, California.

8. Geisler, J.E., 1970: Linear Theory of the Response of a Two Layer Ocean to a Moving Hurricane, Geophysical Fluid Dynamics, 1, pp. 249-272.

9. Gray, W.M., and Shea, D.J., 1973: The Hurricanes' Inner Core Region, 2, Thermal Stability and Dynamic Characteristics, J. Atmos. Sci., 30, pp. 1565-1576.

10. Grigsby, S.H., 1975: The Response of a Two-Layer Hydro-thermodynamic Ocean Model to a Simulated Moving Hurricane, M.S. Thesis, Naval Postgraduate School, Monterey, California.

11. Jordan, C.L., 1964: On the Influence of Tropical Cyclones on the Sea-Surface Temperature Field, Proceedings of the Symposium on Tropospheric Meteorology, N.Z. Meteorol. Serv., Wellington, pp. 614-622.

12. Kraus, E.B., and Turner, J.S., 1967: A One-Dimensional Model of the Seasonal Thermocline, Tellus, 19, pp. 88-106.

13. Leipper, D.F., 1967: Observed Ocean Conditions and Hurricane Hilda, 1964, J. Atmos. Sci., 24, pp. 182-196.

14. Murray, F.W., 1967: On the Computation of Saturation Vapor Pressure, *J. Appl. Met.*, 6, pp. 203-204.

15. Husby, D.M., and Seckel, G.R., 1975: Large Scale Air-Sea Interactions at Ocean Weather Station V, 1951-71, National Oceanic and Atmospheric Administration Report 696.

16. Pollard, R.T., 1970: On the Generation by Winds of Inertial Waves in the Ocean, *Deep-Sea Res.*, 17, pp. 795-812.

17. Pollard, R.T. and Millard, R.C., Jr., 1970: Comparison Between Observed and Simulated Wind-Generated Inertial Oscillations, *Deep-Sea Res.*, 17, pp. 813-821.

18. Price, J.F., 1977: Observation and Simulation of Storm-driven Mixed-Layer Deepening. Rosenthiel School of Marine and Atmospheric Sciences, Technical Report 77-1, University of Miami, 192 pp.

19. Riehl, H., 1963: Some Relations Between Wind and Thermal Structure of Steady-State Hurricanes, *J. Atmos. Sci.*, 20, pp. 276-387.

20. Sheets, R.C., 1974: Unique Data Set Obtained in Hurricane Ellen (1973), *Bulletin of the American Meteorological Society*, 55, no. 2, pp. 144-146.

21. Smith, S.O., and Banke, E.G., 1975: Variation of the Sea Surface Drag Coefficient With Wind Speed, *Quart. J. Royal Met. Soc.,* 101. pp. 665-673.

22. Trapnell, R.N., Jr., 1974: *Ocean Thermal Response to a Moving Hurricane Model*, M.S. Thesis, Naval Postgraduate School, Monterey, California.

23. Tully, J.P., 1953: *Some Characteristics of Sea Water Structure*, Pacific Oceanographic Group, Nanaimo, British Columbia.

24. Withee, G.W., and Johnson, A., 1975: *Data Report: Buoy Observations during Hurricane Eloise*, Data Buoy Office, National Oceanic and Atmospheric Administration.

INITIAL DISTRIBUTION LIST

		No. Copies
1.	Department of Oceanography, Code 68 Naval Postgraduate School Monterey, CA 93940	3
2.	Oceanographer of the Navy Hoffman Building No. 2 200 Stovall Street Alexandria, VA 22332	1
3.	Office of Naval Research Code 410 NORDA, NSTL, Station, MS 39529	1
4.	Dr. Robert E. Stevenson Scientific Liaison Office, ONR Scripps Institution of Oceanography La Jolla, CA 92037	1
5.	Library, Code 3330 Naval Oceanographic Office Washington, DC 20373	1
6.	SIO Library University of California, San Diego P. O. Box 2367 La Jolla, CA 92037	1
7.	Department of Oceanography Library University of Washington Seattle, WA 98105	1
8.	Department of Oceanography Library Oregon State University Corvallis, OR 97331	1
9.	Commanding Officer Fleet Numerical Weather Central Monterey, CA 93940	1
10.	Commanding Officer Naval Environmental Prediction Research Facility Monterey, CA 93940	1
11.	Department of the Navy Commander Oceanographic System Pacific Box 1390 FPO San Francisco 96610	1

12.	Defense Documentation Center Cameron Station Alexandria, VA 22314	2
13.	Library (Code 0212) Naval Postgraduate School Monterey, CA 93940	2
14.	Director Naval Oceanography and Meteorology National Space Technology Laboratories NSTL, Station, MS 39529	1
15.	NORDA NSTL, Station, MS 39529	1
16.	Department Chairman, Code 63 Department of Meteorology Naval Postgraduate School Monterey, California 93940	1
17.	Professor R. L. Elsberry, Code 51Es Department of Meteorology Naval Postgraduate School Monterey, California 93940	5
18.	Professor Warren Thompson Department of Oceanography Naval Postgraduate School Monterey, California 93940	1
19.	LCDR L. Friese, USN FLEWEACEN GUAM COMNAVMARIANAS Box 2 FPO San Francisco 96630	1